Journal of Communications Technology, Electronics and Computer Science, Issue 13, 2017
ISSN 2457-905X

Synthesis and Study of Digital Frequency Modulator-Demodulator

Boyan Karapenev
Department of the Communication Equipment and Technologies
Technical University of Gabrovo
Gabrovo, Bulgaria
bkarapenev@tugab.bg

***Abstract*—This paper presents the synthesis of a digital frequency modulator-demodulator, the design of its main block non-coherent digital frequency demodulator containing a low-pass active filter and an amplitude detector, the performance of simulation studies, implementation of a laboratory model on developed complete technical documentation and presentation of the results obtained by his experimental study.**

Keywords—synthesis; study; digital; frequency; modulator; demodulator

I. Introduction

The transmission of information at long distances is related to the use of modulation and demodulation processes and corresponding devices - modulators and demodulators. Initially, the amplitude, frequency and phase analog modulators/demodulators have found a wide application in practice [7]. The improvement of communications systems in recent years has led to their digitization - of the input information signals, their method of processing and their transmission over the communication channel.

The block diagram of a communication system as shown in Fig. 1. The Transmitter, Receiver and Transmission environment form the so-called Radio channel or Connection channel. Modulators and demodulators are nonlinear devices that in modern duplex communication systems often merge and form a common module – MoDem [8].

The modulation signal in digital modulation $u_{\Omega}(t)$ is a numerical series of logical 0 and logical 1, and the carrier oscillation is sinusoidal and has the form

$$u_H(t) = U_{Hm}\sin(\omega_H t + \varphi_H)\,. \qquad (1)$$

The carrier oscillation parameters in the modulation process change by jumping between two states defined by the digital signal - logical 0 or logical 1. Thus the amplitude, frequency and phase of the carrier oscillation receive discrete values in tact with the modulating digital series. The main types of digital manipulations are: Amplitude Shift Keying – ASK, Frequency Shift Keying – FSK, Phase Shift Keying – PSK and Qadrature-Amplitude Modulation – QAM which is of higher degree.

The modulated signal in frequency manipulation (FSK) is formed as the sum of two ASK signals, each with the corresponding carrier frequency f_{C1} and f_{C2}.

The mathematical model of the modulated FSK signal has the form

$$u_{FSK}(t) = A.\sin(2\pi f_{C1}t) + A\sin(2\pi f_{C2}t)\,. \qquad (2)$$

Its functions are binary and accept only two values - logical 0 or logical 1.

II. Synthesis of Digital Frequency Modulator-Demodulator - a Preliminary Design

The transmitted information from the signal source to the receiver to be transferred over a communication channel requires it to be modulated and accordingly demodulated. The digital frequency modulator-demodulator is designed for signal formation, their transmission - transfer over the communication channel and reception. The connection channel may be a cable or ethereal (terrestrial, satellite).

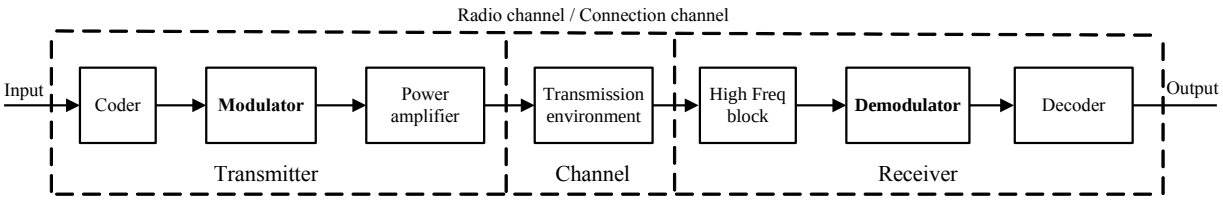

Fig. 1. The block diagram of a communication system.

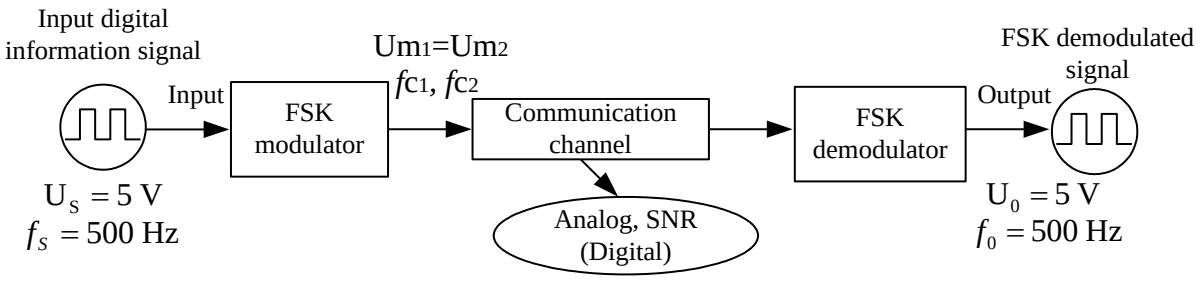

Fig. 2. Block diagram of digital frequency modulator-demodulator.

The block diagram of a digital frequency modulator-demodulator is shown in Fig. 2. The input digital signal into the FSK modulator, the information carrier, is converted to a continuous one, which is transmitted over an analogue connection channel. It is characterized by the following more important parameters and characteristics: Signal-to-Noise Ratio (SNR) and linearity of amplitude and phase responses. The continuous input signal in the FSK demodulator is converted into an output digital signal carrier of the information.

The FSK modulator can be implemented on the basis of various circuit solutions, such as using the widely distributed module-timer 555 or Schmitt-trigger comparator using different capacities to provide a different frequency of the output signal.

In order to ignore the influence of the communication channel it is assumed that the channel is ideal – i.e. there is a direct connection between the FSK modulator and the demodulator.

The FSK demodulator can be [8]:

- built on the basis of a non-coherent scheme, in which direct frequency demodulation of the oscillations is performed;

- differential-coherent, in which the digital series is differentially encoded before performing the frequency manipulation;

- coherent, where synchronous demodulation is performed using an automatic frequency adjustment system. In this case, a specialized PLL integrated circuits (IC) is used;

- implemented with a Digital Signal Processor (DSP).

The implementation of an FSK demodulator with discrete elements, i.e. without the use of specialized IC, DSP and processors, can only be done through a non-coherent scheme [6]. The circuit of a non-coherent FSK demodulator can be synthesized based on the block diagrams in Fig. 3 and Fig. 4 [3].

Non-coherent demodulation of binary FSK modulated signals can be performed by frequency discrimination as shown in Fig. 3. Two parallel-connected circuits transmit one of the two frequencies f_{C1} and f_{C2} and form the amplitudes of the signals from the demodulation performed. The output digital frequency demodulated signal is formed by comparing the two $U_{m1}(t)$ and $U_{m2}(t)$ signals, which can be performed by a comparator.

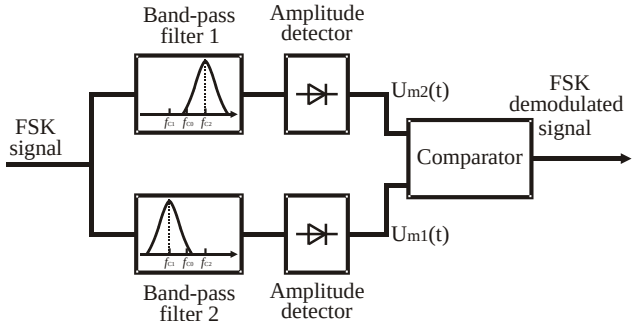

Fig. 3. Block diagram of non-coherent digital frequency demodulator.

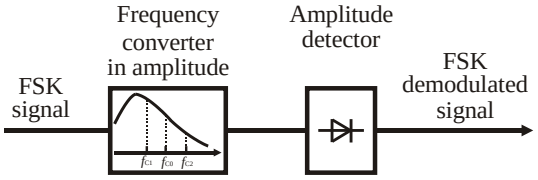

Fig. 4. An non-coherent digital frequency demodulator.

The block diagram of the non-coherent FSK demodulator of Fig. 4 consists of a converter of frequency into amplitude and an amplitude detector. The two frequencies f_{C1} and f_{C2} are in the fall of the amplitude-frequency response (AFR) of low-pass filter or the rising or falling slope of the AFR of band-pass filter for which the voltage transmission coefficient is different. This process is illustrated by the timing diagrams shown in Fig. 5 [3].

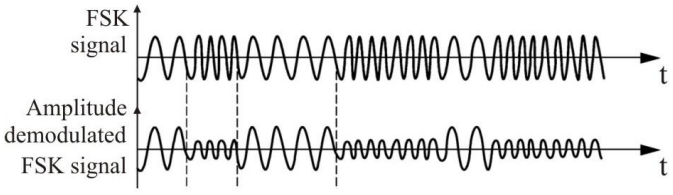

Fig. 5. Time-diagrams of the amplitude-demodulated FSK signal.

In the non-coherent FSK demodulator (Fig. 4), as frequency/amplitude converter, will be used two identical series connected units of low-pass active filters (LPAF) to be able to provide the corresponding voltage transmission coefficients in the course of the AFR for the frequencies f_{C1} and f_{C2}. The output amplitude-demodulated signals should be submitted to a voltage comparator with positive feedback and a hysteresis zone of its switching Ux and the input digital modulation signal carrier of the information appears at the output.

The choice of drop of the amplitude-frequency response of the LPAF used is of great importance. The analytical expression of the transfer function (AFR) is the type

$$T_H(s) = \frac{U_{OUT}}{U_{IN}} = \frac{H_0}{s^n + b_{n-1}s^{n-1} + ... + b_1 s + b_0}, \qquad (3)$$

where U_{OUT} and U_{IN} are respectively the input and output voltages. The steepness of the drop of the AFR outside the overspeed frequency band is determined by the order of the filter. The transmission coefficient H_0 does not depend on the type of LPAF but on its schematic implementation and is involved in determining the transmission coefficient T_{0H} of the low-pass filter at the frequency $f = 0$ ($T_{0H} = H_0/b_0$).

The most appropriate choice of the unit of LPAF - from I order and polynomials and ratios of II order with different quality factor Q is between a Sallen-Key topology filter and a II order unit(s) with a quality factor from 10 to 50.

Since the Sallen-Key Low-pass units have a simpler configuration and implementation as well as the design they are chosen when building the FSK demodulator.

III. Design of Digital Frequency Modulator-Demodulator. Simulation Results

Design and studies of digital frequency modulators - using Module-timer 555 and Schmitt-trigger are presented in [4] and [5] respectively.

A. Design of the Sallen–Key Filter from the Structure of the Digital Frequency Demodulator

The active filters by Sallen-Key topology are some of the most commonly used in practice because of the simple construction and the good quality parameters and characteristics which they provide. They are built using an active element (operational amplifier), two series connected resistors R1 and R2 (R3, R4) to the non-inverting input and two capacitors C1 and C2 (C3, C4) – Fig. 6 [1].

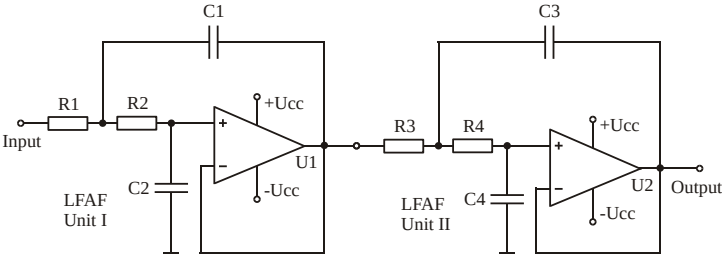

Fig. 6. Low-pass active filter by Sallen-Key topology.

The transfer function $T_H(s)$ of such a filter is of the type

$$T_H(s) = \frac{U_{OUT}(s)}{U_{IN}(s)} = \frac{\frac{1}{R1.C1.R2.C2}}{s^2 + s\left(\frac{1}{R2.C2} + \frac{1}{R1.C1}\right) + \frac{1}{R1.C1.R2.C2}} \qquad (4)$$

where U_{OUT} and U_{IN} are the input and output voltages respectively, and s - complex variables.

The design of the low-pass unit by Sallen-Key topology can be done with the electronic web-calculator [1]. For input data R1 = R2 = 10 kΩ, C1 = 10 nF and C2 = 1 nF the following more important results are obtained:

Transfer function	$T_H(s)$	$T_H(s) = \frac{10^9}{s^2 + 2.10^4.s + 10^9}$;
Cut-off frequency	f_C	5032,92121 Hz;
Quality factor	Q_{PH}	1,5113883;
Attenuation ratio	ξ	0,316227766.

The design of the low-pass unit by Sallen-Key topology can be performed in the following simplified sequence [2]:

- set the cut-off frequency – f_C = 5 kHz;
- the value of the capacitor C2 is chosen within the range of 100 pF ÷ 100 nF. In this case C2 = 1 nF;
- determine the value of C1 = (1 ÷ 10).C2, as C1 = 10.C2 = 10 nF;
- calculate the values of R1 и R2 by dependence

$$R1 = R2 = \frac{0{,}707}{2.\pi.f_C.(2.C2)}. \quad (5)$$

For resistors R1 and R2 standard values of 10 kΩ each are selected.

B. Design of the Amplitude Detector from the Structure of the Digital Frequency Demodulator

U_{RL1} = 3,7 V is accepted for logical 1 and U_{RL2} = 1,8 V is accepted for logical 0 for the reference levels (RL) defining the hysteresis of Schmitt-trigger. Its width is obtained $U_X = U_{RL1} - U_{RL2}$ = 1,9 V. With a selected value of R13 = 10 kΩ in equations (6) is compiled a system of two equations with two unknowns from which the resistance of resistors R15 2948 Ω и R14 4396 Ω is determined. Their default values are chosen accordingly 3 kΩ and 4,3 kΩ (Fig. 7).

$$U_{RL1} = \frac{R14}{R14 + R13 \| R15}.U_{CC} \text{ and } U_{RL2} = \frac{R14 \| R15}{R13 + R14 \| R15}.U_{CC} \quad (6)$$

Since the designed FSK demodulator can be simulated only in the structure of the synthesized FSK modulator-demodulator (Fig. 2) and in Fig. 7 presents the circuit for its simulation study. It also contains the FSK modulator and two units by Sallen-Key topology.

The oscillogram of signals in nodes 4 (FSK modulated signal) and 16 - after both low-pass units are shown in Fig. 8. The latter appears to be the input for the FSK demodulator (U4). The obtained oscillogram of the signals in nodes 4 (FSK modulated signal) and 21 - after the FSK demodulator is presented in Fig. 9.

Since the output signal of the comparator of the FSK demodulator continuously switches with the frequency of the amplitude demodulated signal with the greater amplitude (Fig. 9) available at logic 1 of the input modulation signal which requires its smoothing. For this purpose, the structure of the FSK demodulator envisages the use of a full-wave rectifier D1 (Graetz circuit) and a pulsating smoothing capacitor C8, in which case both intermediate signals of different amplitude are rectified – Fig. 11.

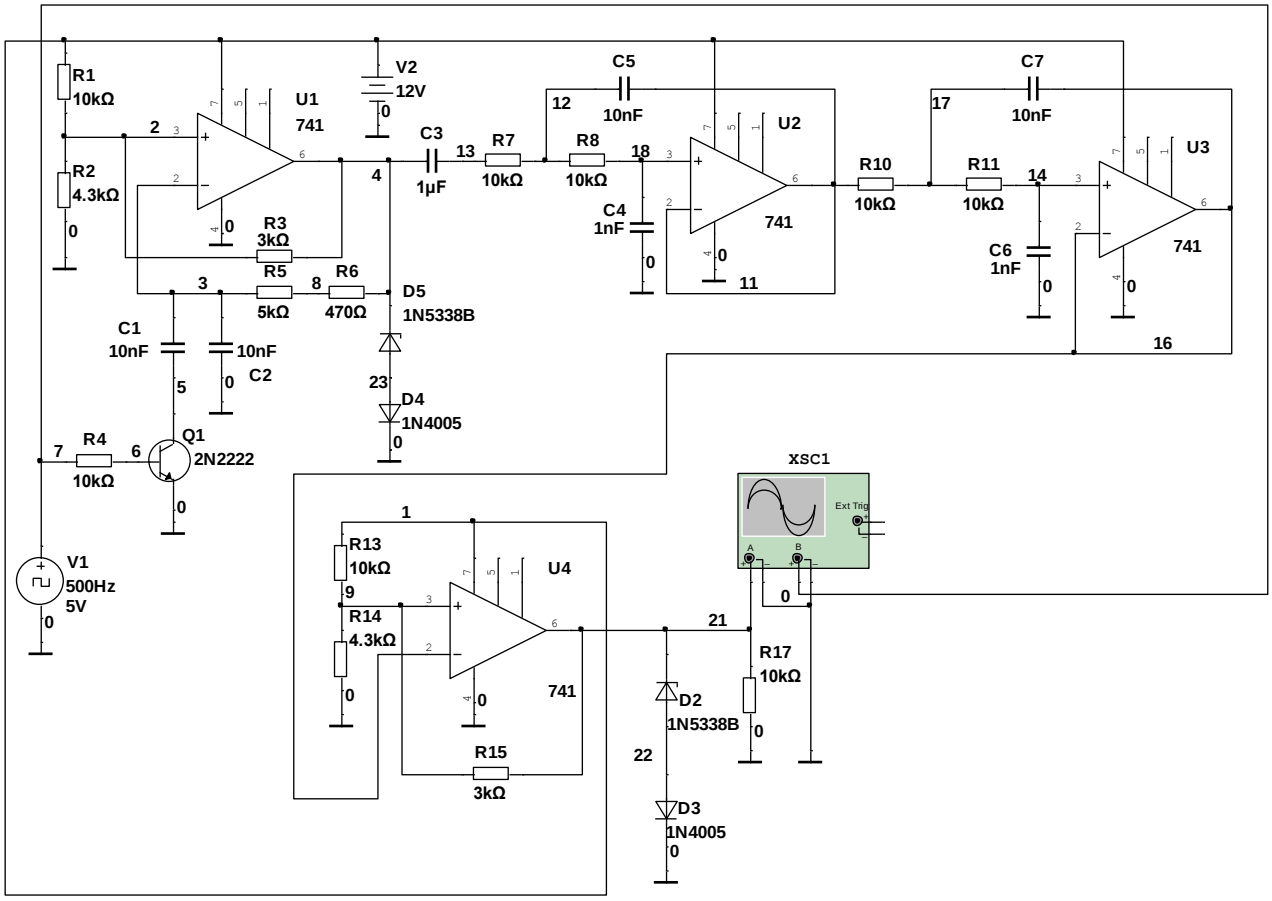

Fig. 7. Circuit for simulation study of the synthesized FSK modulator-demodulator.

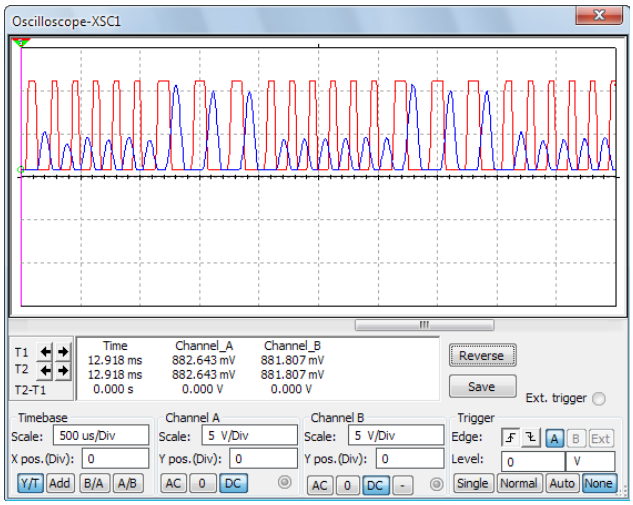

Fig. 8. An oscillogram of the FSK modulated signal (node 4) and filtered after the two series connected LPAF (node 16).

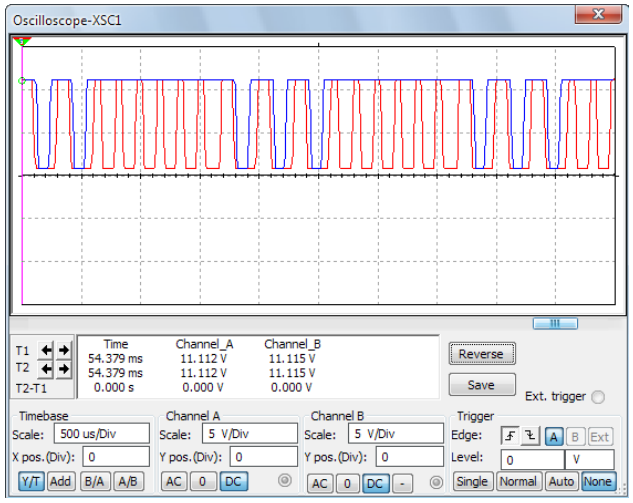

Fig. 9. An oscillogram at the input and output of the synthesized FSK modulator-demodulator.

The complete schematic circuit of the synthesized FSK modulator-demodulator containing the Graetz rectifier and an inverter at the output of the FSK demodulator since the output signal is dephased at approximately 180º is shown in Fig. 10.

The obtained oscillogram of the FSK modulated signal (node 4) and the rectified node 20 after Graetz rectifier (Fig. 10) is shown in Fig. 11.

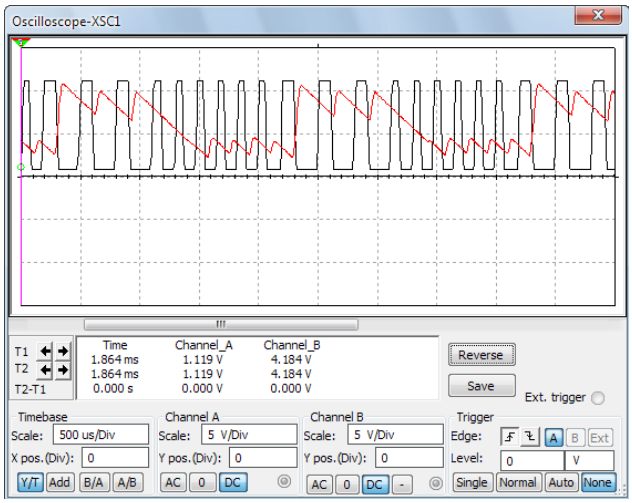

Fig. 11. An oscillogram of the FSK modulated signal (node 4) and the rectified node 20 after Graetz circuit.

The presence of a Graetz rectifier circuit in the FSK demodulator structure changes the DC signal levels for frequencies f_{C1} and f_{C2}. In this case, the reference levels defining the hysteresis of Schmitt-trigger for the FSK demodulator assume values U_{RL1} = 6,5 V for logic 1 and U_{RL2} = 5,5 V for logic 0. This requires a recalculation of the values of the elements R13, R14 and R15 (Fig. 10), as a result of which the value of hysteresis Ux is changed. At the selected value of R13 = 500 Ω in equations (6), after solving the system of two equations with two unknowns, the resistances of resistors R14 490 Ω and R15 3096 Ω are determined. For their standard values are selected respectively 500 Ω and 3 kΩ.

The simulated oscillogram at the input and output of the synthesized FSK modulator-demodulator (Fig. 10) is shown in Fig. 12.

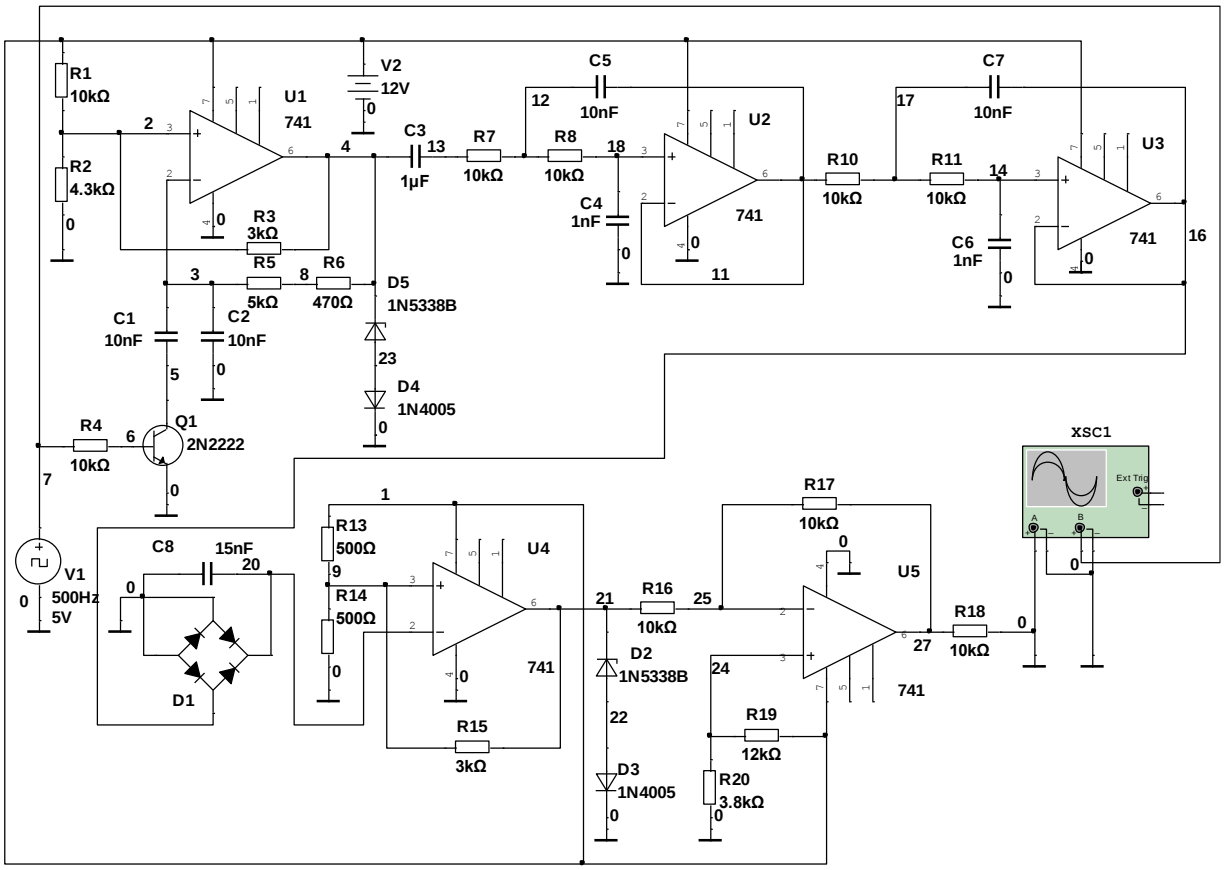

Fig. 10. The complete circuit of the synthesized FSK modulator-demodulator.

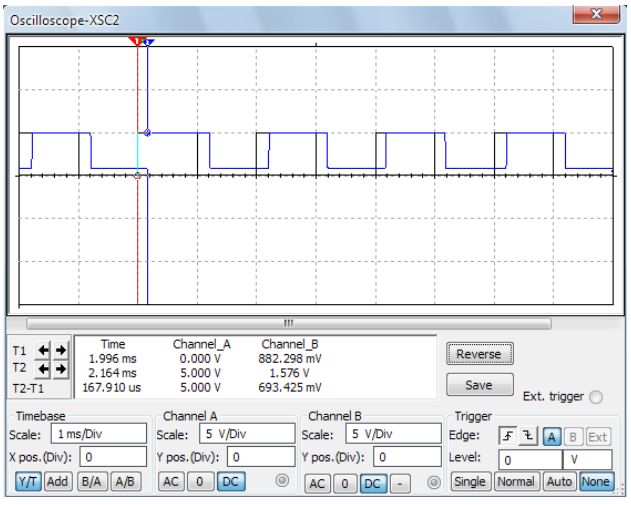

Fig. 12. An oscillogram of the input and output signals of the synthesized FSK modulator-demodulator.

IV. Experimantal Studies of Designed Digital Frequency Modulator-Demodulator

Table 1 presents the measured DC voltages in the respective nodes since some of the FSK modulator-demodulator circuits have a DC operating mode, for example, the reference levels (voltages) of the non-inverting inputs of the Schmitt-triggers U1, U4 and inverter U5 (nodes 2, 9 and 24 in Fig. 10). They are compared to the simulated ones and the relative error between them is determined.

TABLE I. DC Operating Point of the FSK Modulator-Demodulator

Node	2	9	24
Usimulation, V	3,60	5,95	2,89
Uexperimental, V	4,39	5,67	2,89
ε, %	18	4,9	0

The experimentally obtained oscillograms in the specified nodes of the FSK modulator-demodulator synthesized circuit (Fig. 10) are shown in Figures 13 ÷ 16. A generator is connected to the input of the circuit and the signal is bi-polar with square pulses with amplitude 4 V and frequency 500 Hz - Fig. 13.

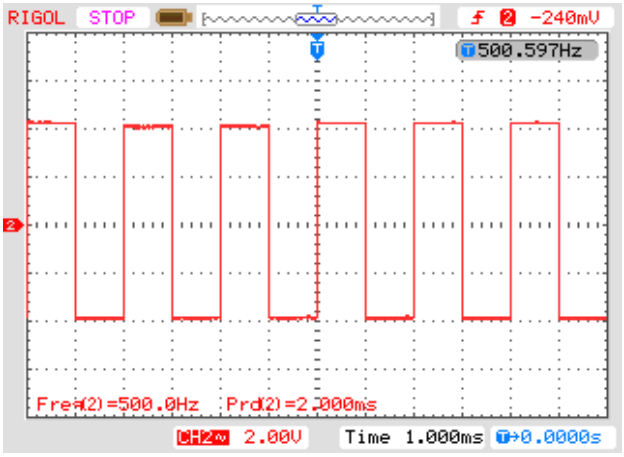

Fig. 13. An oscillogram of the input digital modulation signal - node 7.

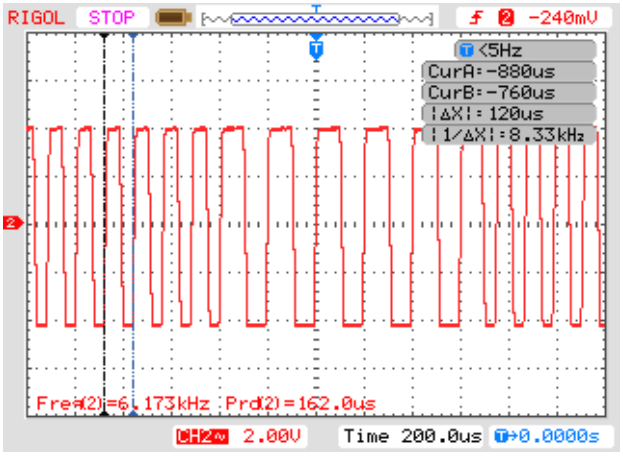

Fig. 14. An oscillogram of output signal of FSK modulator at logic 0 with f_{C2} = 8,33 kHz - node 4.

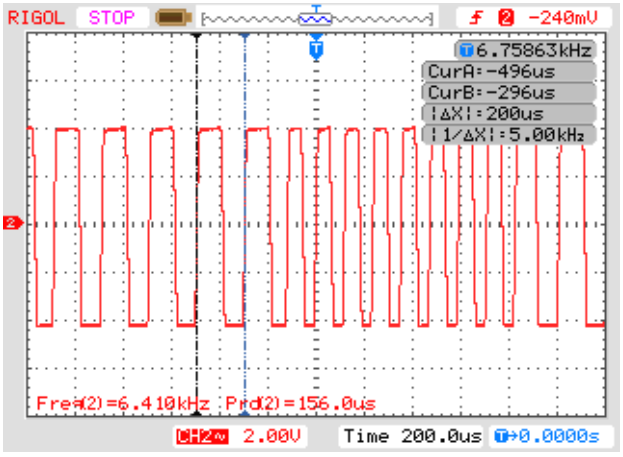

Fig. 15. An oscillogram of output signal of FSK modulator at logic 1 with f_{C1} = 5 kHz - node 4.

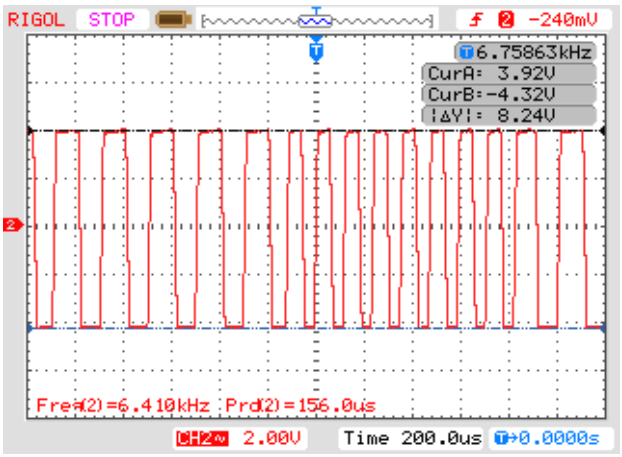

Fig. 16. An oscillogram of output signal of FSK modulator - amplitude value - node 4.

After passing the input signal to the comparator (U1 in Fig. 10) at the output a signal with two different frequencies is obtained as frequency f_{C1} is 5 kHz - Fig. 14, and f_{C2} is 8,33 kHz - Fig. 15. The measured peak to peak voltage is shown in Fig. 16 and has a value of 8,24 V and it has positive polarity of 3,92 V and negative of -4,32 V. After converting the input digital signal into a modulated FSK, it enters the low-pass active filters to provide different amplitudes for frequencies f_{C1} and f_{C2}. The obtained oscillograms of the LPAF with one unit are shown in Figures 17 ÷ 20. U_{pp} of signal is 8,64 V for frequency f_{C2} (Fig. 17) and for f_{C1} - 5,04 V – Fig. 18. The periods of frequencies f_{C1} and f_{C2} were determined by the experimental studies shown in Figures 19 and 20, as for frequency f_{C2} ΔT = 200 µs - Fig. 19 and for frequency f_{C1} ΔT = 120 µs - Fig. 20.

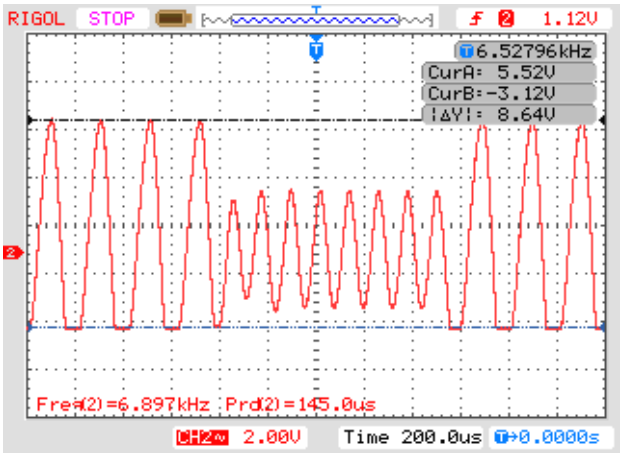

Fig. 17. An oscillogram of the output of LPAF 1 with ΔY_{C1} = 8,64 V - node 11.

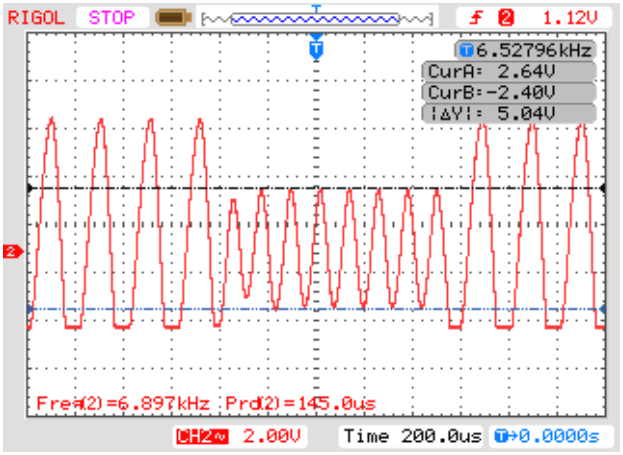

Fig. 18. An oscillogram of the output of LPAF 1 with ΔY_{C2} = 5,04 V - node 11.

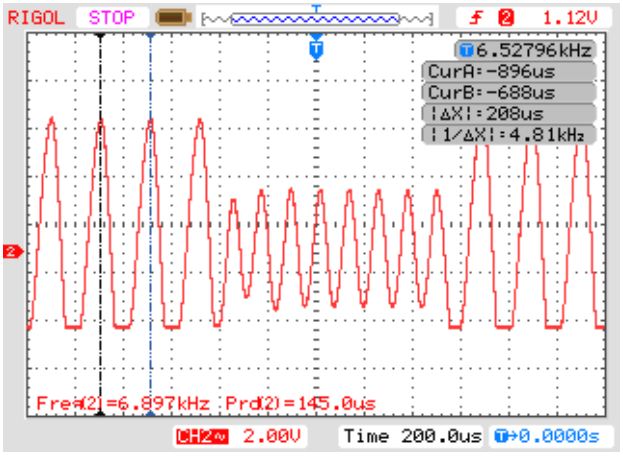

Fig. 19. An oscillogram of the output of LPAF 1 with $\Delta X_{C1} \approx 5$ kHz, ΔT = 200 µs – node 11.

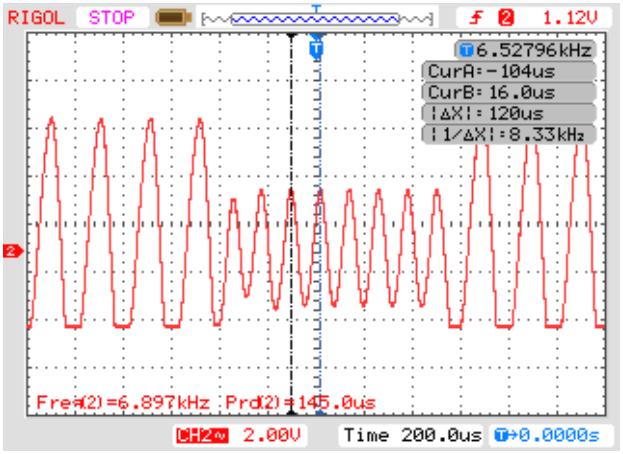

Fig. 20. An oscillogram of the output of LPAF 1 with ΔX_{C2} = 8,33 kHz, ΔT = 120 µs – node 11.

After the filtration of the first LPAF, the signal enters the second unit for second filtration and provides the necessary amplitudes for frequencies f_{C1} and f_{C2}. The oscillograms of the LPAF can be compared and determine the differences in the signals between the first unit shown in Figures 17 and 18, and the second - Figures 21 and 22. Voltage drop after the second filter is approximately 5 V.

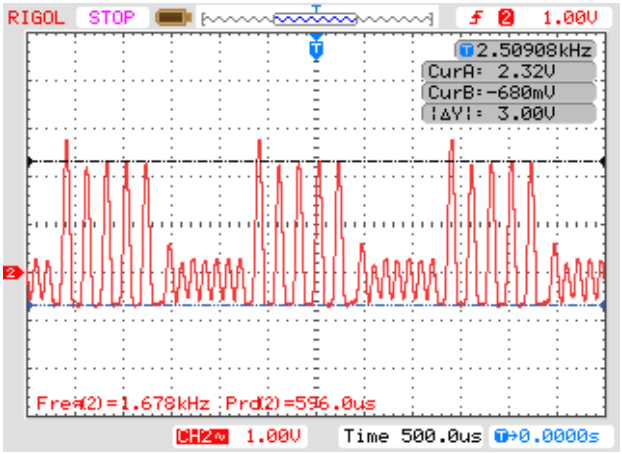

Fig. 21. An oscillogram of the output of LPAF 2 with ΔY_{C1} = 3 V - node 16.

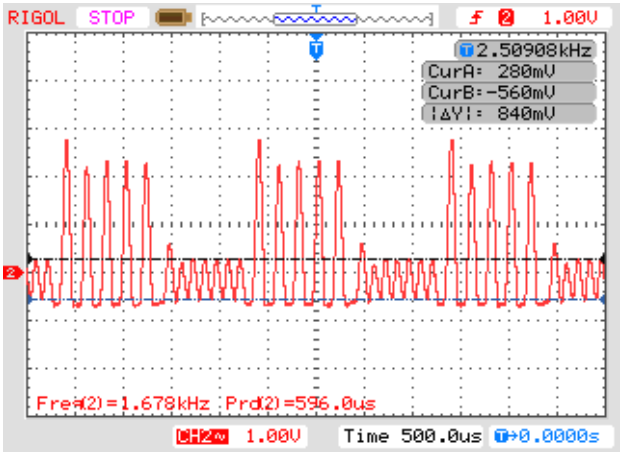

Fig. 22. An oscillogram of the output of LPAF 2 with ΔY_{C2} = 0,84 V - node 16.

The oscillograms from which were measured the frequencies and the time-intervals of following the signals after the LPAF with two units are shown in Figures 23 and 24. The measured values fully match those of the LPAF with one unit shown in Figures 19 and 20.

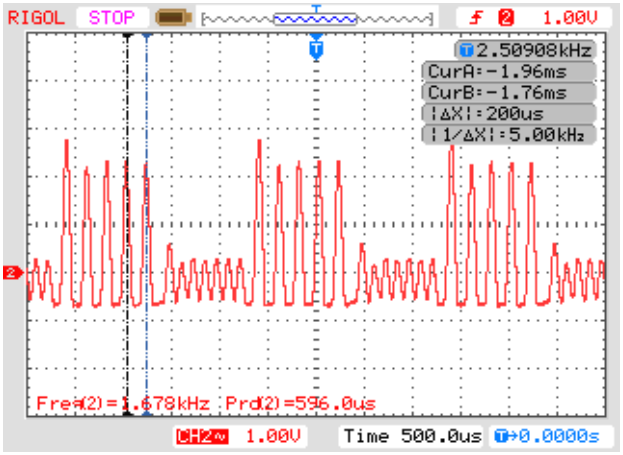

Fig. 23. An oscillogram of the output of LPAF 2 with ΔX_{C1} = 5 kHz, ΔT = 200 μs – node 16.

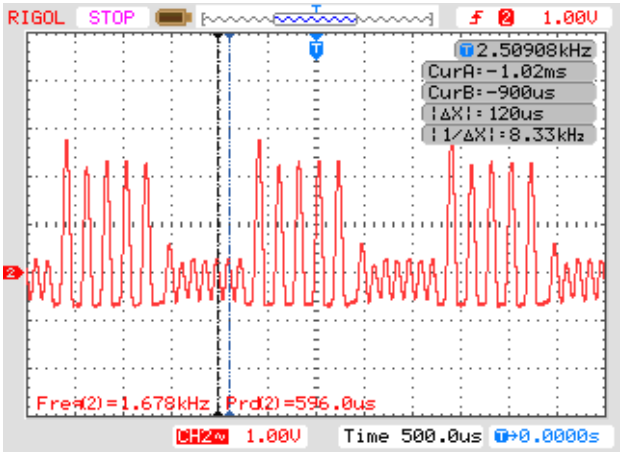

Fig. 24. An oscillogram of the output of LPAF 2 with ΔX_{C2} = 8,33 kHz, ΔT = 120 μs – node 16.

Summary

The behavior of the synthesized circuit of a non-coherent digital frequency modulator-demodulator during the simulation and experimental studies is analogous while preserving the form and character of the intermediate signals in the individual nodes. However, there are minimal differences in both the operating frequencies and the amplitudes of the intermediate signals.

V. Conclusion

The synthesis of a digital frequency modulator-demodulator is related to the development of a preliminary design in which are presented the requirements for the individual component blocks and the possibilities for their choice and implementation. The design, simulation, and experimental study of a digital frequency modulator with a timer-module 555 and a Schmitt-trigger has been carried out. Among the choices of FSK demodulator - coherent, differential-coherent and non-coherent, the latter is chosen because its implementation is not related to the use of specialized integrated circuits such as PLL and DSP. It was synthesized by LPAF - a two Sallen-Key topology units and an amplitude detector (Schmitt-trigger comparator). The simulation and experimental studies were performed for all composite modules as well as for the entire synthesized non-coherent digital frequency modulator-demodulator by presenting the results obtained which visualize the processes in progress.

The presented synthesis, design and the obtained simulation and experimental results illustrate the work and explain the principle of operation of the synthesized circuit of a digital frequency modulator-demodulator. They could also be used in the design, simulation and experimental study of other circuits widely used in communications and practice.

Analogously, other types of modulators, demodulators, as well as other similar circuits can be synthesized, designed, implemented, simulated and experimentally studied.

References

[1] Sallen-Key Low-pass Filter Design Tool, Okawa Electric Design, http://sim.okawa-denshi.jp/en/ OPseikiLowkeisan.htm, 2017.

[2] Sallen-Key Low-pass Filter, eCircuit Center, http://www.ecircuitcenter.com/Circuits/opsalkey1/ opsalkey1.htm, 2017.

[3] Thierry Taris, Hassène Kraimia, Didier Belot and Yann Deval, An FSK and OOK Compatible RF Demodulator for Wake Up Receivers, Journal of Low Power Electronics and Applications, ISSN 2079-9268, pp. 276-277, November 2015, www.mdpi.com/journal/jlpea

[4] B. Karapenev, "A digital frequency modulator using module-timer 555", Scientific papers at the University of Rousse, Volume 54, Series 3.2, ISSN 1311-3321, pp. 41-46, 2015, http://conf.uni-ruse.bg/bg/docs/cp15/3.2/3.2-6.pdf

[5] B. Karapenev, "A digital frequency modulator using Schmith-trigger", Scientific papers at the University of Rousse, Volume 54, Series 3.2, ISSN 1311-3321, pp. 92-98, 2015, http://conf.uni-ruse.bg/bg/docs/cp15/3.2/3.2-14.pdf

[6] B. Karapenev, "Macromodel synthesis of digital non-coherent frequency demodulator and simulation studies of FSK modulator-demodulator", Journal of the Technical University of Gabrovo, volume 54, ISSN 1310-6686, pp. 45-48, 2017.

[7] D. Dobrev, L. Yordanova, Radiocommunications, parts one and two, Publishing house SIELA, Sofia, respectivelly 2001 and 2003.

[8] I. Nemigenchev and B. Karapenev, Communication Transform Devices, University Publishing House "Vasil Aprilov", ISBN 978-954-683-361-7, Gabrovo, 2007.